Rapid directional changes associated with a 6.5 kyr-long Blake geomagnetic excursion at the Blake-Bahama Outer Ridge.

Mark Bourne[a,1], Conall Mac Niocaill[a], Alex L. Thomas[a], Mads Faurschou Knudsen[b], Gideon M. Henderson[a]

[a] *Department of Earth Sciences, University of Oxford, South Parks Road, Oxford OX1 3AN, United Kingdom*
[b] *Department of Earth Sciences, Århus University, Høegh-Guldbergs Gade 2, 8000 Århus C, Denmark*

Abstract

Geomagnetic excursions are recognised as intrinsic features of the Earth's magnetic field. High-resolution records of field behaviour, captured in marine sedimentary cores, present an opportunity to determine the temporal and geometric character of the field during geomagnetic excursions and provide constraints on the mechanisms producing field variability. We present here the highest resolution record yet published of the Blake geomagnetic excursion (∼125 ka) measured in three cores from Ocean Drilling Program (ODP) Site 1062 on the Blake-Bahama Outer Ridge. The Blake excursion has a controversial structure and timing but these cores have a sufficiently high sedimentation rate (∼10 cm ka^{-1}) to allow detailed reconstruction of the field behaviour at this site during the excursion. Palaeomagnetic measurements of the cores reveal rapid transitions (< 500 years) between the

Email address: mark.bourne@earth.ox.ac.uk (Mark Bourne)
[1]Corresponding author. Tel.: +44 0 1865 272 001; fax: +44 0 1865 272 072

contemporary stable normal polarity and a completely reversed state of long duration which spans a stratigraphic interval of 0.7 m. We determine the duration of the reversed state during the Blake excursion using oxygen isotope stratigraphy, combined with ^{230}Th excess measurements to assess variations in the sedimentation rates through the sections of interest. This provides an age and duration for the Blake excursion with greater accuracy and with constrained uncertainty. We date the directional excursion as falling between 129 and 122 ka with a duration for the deviation of 6.5±1.3 kyr. The long duration of this interval and the fully reversed field suggest the existence of a pseudo-stable, reversed dipole field component during the excursion and challenge the idea that excursions are always of short duration.

Keywords:
paleomagnetism, geomagnetism, geomagnetic excursion, Blake, 230Th, ODP (Ocean Drilling Program)

---

1. Introduction

Palaeomagnetic measurements have revealed that since the last full reversal the Earth's magnetic field has, for brief intervals, deviated from the behaviour expected during 'normal' secular variation (Laj and Channell, 2007). These significant deviations in direction and intensity of the Earth's field have become known as geomagnetic excursions. While geomagnetic excursions have long been recognised in palaeomagnetic records (e.g. Channell, 2006; Lund et al., 1998; Laj et al., 2006) the mechanism that causes them and their relationship to reversals remain enigmatic (Merrill and McFadden, 1999; Roberts, 2008). The durations of excursions are of particular interest

because they may relate to the stability of magnetic field states and provide information about processes during directional changes in the field.

For instance, Gubbins (1999), expanding on work by Hollerbach (1993), proposed a hypothesis to explain why the field rapidly returned to its original polarity following an excursion, rather than remain in the opposite state, as in a reversal. The hypothesis emphasized the influence of interactions between the inner and outer core on the geomagnetic field, whereby the inner core imposes a magnetic inertia on the system. Gubbins (1999) suggested that an excursion, in contrast to a full reversal, occurs when the magnetic field in the liquid outer core does not persist in a reversed state for sufficient time for the solid inner core's field to also achieve reversal. The implication is that the duration of excursions should be relatively short ($\sim$3 kyr); otherwise the inner core would stabilise the reversed polarity interval, resulting in a long-duration (10s-100s kyr) chron. By understanding excursions and their relation to full reversals, we can test this hypothesis, and more generally, gain insight into processes in the Earth's core and the causes of variation in the Earth's field.

Detailed analyses of recent geomagnetic excursions have tried to determine typical durations for excursions. Two of the most recent have been studied in particular detail. The Laschamp excursion (LE) ($\sim$41 ka), first identified in the Laschamp and Olby lava flows in central France (Bonhommet and Babkin, 1967), has since been found in globally distributed marine core records and is now generally recognised as being of relatively short duration ($\sim$2 kyr) (Channell, 2006; Laj et al., 2000, 2006).

Initial studies suggested that the duration of the earlier, Iceland Basin

excursion (IBE) (∼185 ka) might also be relatively short (∼2 kyr) (Laj et al., 2006). However, using a novel geochemical approach to capture variations in sedimentation rate in cores from the North Atlantic, Knudsen et al. (2007) demonstrated that the IBE had a longer duration of up to 7 kyr, apparently challenging the idea that excursions would have a short duration.

The difference in duration for these two excursions and the limited number of excursions studied at sufficiently high resolution, leaves unclear whether excursional events have a characteristic duration. The rate at which the Earth's field changes direction, and thus the time taken for the field to reverse, is an additional constraint on the nature of fluid flow in the outer core that generates the geomagnetic field.

A virtual geomagnetic pole (VGP) does not necessarily represent a true magnetic pole, rather it is calculated on the assumption that the magnetic field direction at a location is the result of a dipolar field. The rate at which the VGP 'moves' should therefore be understood as a representation of the rate of change of the field direction at the site location rather than the movement of any 'real' pole.

Clement (2004) presented an analysis of records of the last four geomagnetic reversals that estimated the mean time taken for the VGP to reverse. the duration of the transition zones was found to be 5 ± 1 kyr, corresponding to a rate of latitudinal change of 18° kyr^{-1} (where the transition zone is defined as the period within which the VGP was between 45°N and 45°S).

However, the rate of change of field direction appears to be significantly faster during excursions. By virtue of the short duration of the Laschamp excursion, during which VGPs from some records reach latitudes beyond

45°S (Laj et al., 2006), the sum of the two transition intervals must be less than 2 kyr. This implies rates of VGP change of at least 90° kyr^{-1}; a rate significantly faster than for reversals. The records of the IBE presented by Knudsen et al. (2007), suggest minimum transition rates of ∼30° kyr^{-1}, where transitions take 3 kyr, from a core on the Gardar Drift but far more rapid transition rates of ∼200° kyr^{-1} from a core on the Bermuda Rise. While geometric effects could potentially account for some of the discrepancy between the excursional and full reversal transition rates, the difference is sufficiently great to suggest that polarity transitions may be more rapid during excursional events than during full reversals.

2. The Blake Excursion

The Blake excursion was first documented by Smith and Foster (1969) in seven deep-sea sediment cores from the Blake Outer Ridge in the western North Atlantic. It has since become commonly accepted as a global geomagnetic feature occurring between the Laschamp and Iceland Basin excursions (Laj and Channell, 2007). However, whilst the Blake excursion is represented in many cores and palaeomagnetic records it remains one of the most ambiguous of the recent geomagnetic excursions. What is clear though is that, like other polarity transitions, the Blake excursion is associated with an interval of significantly reduced geomagnetic field intensity. Global relative palaeointensity stacks reveal a long duration interval of reduced palaeointensity lasting (∼25 kyr), demonstrating that the excursion is an intrinsic feature of the global field (Frank et al., 1997; Valet et al., 2005; Channell et al., 2009; Ziegler et al., 2011).

Previous studies of the timing and duration of the Blake event are compiled in Table 1. Although the field intensity is well-constrained, estimates for the duration and timing of any directional deviation during the Blake excursion vary and the uncertainties are unconstrained. Radiometric dating of lavas suggest reversed directions at 123±7 ka (Zhu et al., 2000) and a reef carbonate record places the beginning of a reversed event at 132.8±1.3 ka (Ménabréaz et al., 2010) (Table 1). Tric et al. (1991) provide one of the most detailed marine records of a 'Blake' event (Fig. 1a), identifying a double event in a core from the Nile River Fan in the Eastern Mediterranean (following work by Tucholka et al. (1987)). Using oxygen isotope stratigraphy and tephrochronology, Tric et al. (1991) found the event within marine isotope stage (MIS) 5e and calculated an upper bound for the excursion's duration of 4.5 kyr.

However, even within the Mediterranean, cores suggest durations ranging from 3.5–8.6 kyr (Tucholka et al., 1987). This discrepancy is most likely the result of three factors: the potential for unrecognised variations in sedimentation rates between widely spaced age-constrained boundaries and the combined effects of limited resolution and significant magnetic remanence lock-in depths at low-sedimentation rates (< 10 cm kyr^{-1}) (Roberts and Winklhofer, 2004). Palaeomagnetic records from cores on the Yermack Plateau in the Arctic suggested a relatively long duration of up to ∼10 kyr (Nowaczyk et al., 1994). However, these Arctic sediments have since been identified as potentially subject to a chemical remanent magnetization (CRM) that can result in self-reversal (Channell and Xuan, 2009) and thus these records are potentially unreliable.

Some of the previous records that suggest the most complex field be-

haviour during the Blake excursion, such as those of Zhu et al. (1994) and Fang et al. (1997), have been obtained from sections from the western Loess Plateau of China (Fig. 1b and c). In both of these records, the Loess appears to record multiple reversed periods with an estimated total duration of $\sim$5 kyr. Yet dating loess records is not trivial; age models for loess rely on thermoluminescence dating and correlating palaeosol horizons and magnetic parameters with global isotope curves (e.g. Kukla et al., 1988; Evans and Heller, 2001; Fang et al., 1997). The limited resolution of age models means that average sedimentation rates are used over relatively long intervals.

As noted by Parés et al. (2004), on examination the two Loess records are significantly different. Most importantly, the reversed directions appear in different stratigraphic horizons in the sections. Zhu et al. (1998) and Parés et al. (2004) demonstrated that there are ambiguities in the faithfulness of loess palaeomagnetic records of the Blake excursion after failing to find the event in many sections in the Chinese Loess Plateau. Parés et al. (2004) attribute the absence of the event to delayed magnetization acquisition and a previously unrecognised CRM. In the face of these difficulties and inconsistencies, it is hard to be confident in either of the two loess records of the Blake and the field behaviour they describe.

Excursional field behaviour during the Blake excursion therefore remains ambiguous. A coherent global picture of the excursion is limited by the quality of previous records and the difficulties in dating marine records. It is difficult to discern whether previously observed anomalous directions within this period of low field intensity correspond to a global directional excursion feature or represent localised fluctuations apparent during a period of reduced

dipole intensity.

3. Study Site and Sampling

We present a new palaeomagnetic record of the Blake excursion, at the highest resolution yet achieved, using discrete samples obtained from Ocean Drilling Program (ODP) Site 1062 on the Bahama Outer Ridge (Fig. 2a, 28° 14.8'N, 74° 25.0'W). ODP Leg 172 has been invaluable in demonstrating the existence of multiple excursions during the Brunhes chron (Lund et al., 1998, 2001). Using published shipboard long-core measurements for ODP Leg 172 (Shipboard Scientific Party, 1998a), three cores from the Bahama Outer Ridge were selected for this study (Site 1062, Cores B, D and E). We derive a new high resolution chronology for the Blake excursion at Site 1062 using $^{230}\mathrm{Th}_{xs}$ measurements coupled to an oxygen isotope stratigraphy.

Discrete cubic samples ($\sim$7 cm^3 sample volume) were taken from the three cores at the ODP repository in Bremen. In all, 78 samples were taken from core 1062B (16.25–25.40 mbsf), 157 from 1062D (10.37–34.08 mbsf) and 151 from 1062E (8.50–27.53 mbsf). Within the excursional interval, sampling was undertaken at 2.5 cm intervals so that this record is virtually continuous. Considering the average sedimentation rate ($\sim$10 cm kyr^{-1}) the individual samples represent an average of 200 years.

4. Age Model

4.1. Composite Depth Scale

Although the three cores at Site 1062 are close to one another, gaps in recovery mean that a composite depth scale is required to compare equiva-

lent intervals between them. The procedure employed shipboard to develop a composite depth scale links the cores using constant depth offsets at selected tie-points. (Shipboard Scientific Party, 1998b). However, the limitation of using linear depth offsets is that not all prominent features within the individual cores are aligned. Within the interval studied here, correlation of decimetre-scale features in the shipboard magnetic susceptibility record was found to be poor. Thus, to determine the precise relationship between samples in neighbouring cores, we have developed a more refined correlation across the studied interval. A new cross-correlation of the cores was created by comparing records of three sedimentological parameters measured shipboard that are independent of magnetic field direction: L*, a measure of the lightness of the sediment; gamma ray count; and magnetic susceptibility. Features in cores 1062B and D are correlated to those in 1062E. All subsequent depths from 1062B, D and E are quoted in 'revised metres composite depth' (rmcd) which is their equivalent depth in 1062E (mbsf). Note therefore, that for 1062E, 'rmcd' is the same as 'mbsf'.

4.2. Oxygen Isotope Stratigraphy

Age models for the cores exist from shipboard and later work but have been refined by two separate approaches for this study. In the absence of isotope data, Grützner et al. (2002) derived age models for the cores at Site 1062 by tuning variations of estimated carbonate content to the orbital parameters. Although variations in carbonate content show a first-order trend associated with glacial-interglacial cycles for some Leg 172 sites (Chaisson et al., 2002), variance in sedimentological parameters may be affected by local, rather than global, factors.

To refine the chronology, we use two separate approaches for this study. We have cross-correlated Core 1062E with a benthic δ^{18}O record in a neighbouring piston core, Knorr 31 GPC9 (28°14.7'N, 74°26.4'W, 4758 m) (Keigwin et al., 1994) and measure a planktic δ^{18}O record in Core 1062E itself.

We correlate Core 1062E with Knorr 31 GPC9 using the variations in estimated carbonate content derived from diffuse spectral reflectance (Giosan et al., 2001). GPC9 has a measured carbonate content record and a measured oxygen isotope record from analyses of benthic foraminifera *Cibicidoides* spp. (Keigwin et al., 1994) (Figure 2b). On the basis of our correlation between the two cores, the GPC9 benthic δ^{18}O record is placed on the 1062E depth scale in Figure 2c.

To further confirm this δ^{18}O chronology, we also measured the oxygen isotopes of planktonic foraminfera from Core 1062E. Following magnetic analysis, each sample was submerged in deionised water and mechanically agitated until suspension of the sediment was achieved. The sediment suspension was then sieved and the 63 μm fraction retained. This fraction was subsequently dried in an oven at 50°C. Specimens of the planktonic *Globorotalia inflata* were the most consistently present species throughout the studied core interval and were therefore chosen for analysis. Benthic foraminifera were rare. Due to the small volume of sediment per sample ($\sim$7 cm^3), only a limited number of samples contained sufficient specimens for analysis. Oxygen isotope analyses were conducted using a Kiel IV attached to a Delta V isotope ratio mass spectrometer at the University of Oxford. All measurements are given in standard delta notation in per mil (‰) relative to the Vienna PeeDee Belemnite (V-PDB) carbonate standard. Isotopic values were related to the

V-PDB standard by repeated measurements of National Bureau of Standards NBS-19 and NBS-18 (with δ^{18}O values of -2.2‰ and -23.2‰ respectively). Analytical precision for replicate standard measurements (n=13) of δ^{18}O in NBS-19, made concurrently with 1062E analyses, was ±0.09‰ (1σ).

In total, 53 samples from 1062E were analysed. Three well-preserved specimens of *G. inflata* were used for each stable isotopic measurement and 10 samples were repeated to check the reproducibility of the results and assess the potential for seasonal bias. Two measurements, at 12.73 and 14.78 rmcd, were identified as anomalous and are probably the result of diagenetic alteration of fractured shells. These measurements were disregarded from further analysis. The results of our δ^{18}O analysis are shown in Figure 2c.

4.3. Chronology

Biostratigraphy conducted during the ODP expedition identified the last appearance of *Globorotalia tumida flexuosa* (68 ka) to be at a minimum depth of 13.23 rmcd in core 1062E (Shipboard Scientific Party, 1998a). Using this biostratigraphic datum as a guide, we correlate the GPC9 and 1062E oxygen isotope curves to the global record.

We derive two age-constrained boundaries (Fig. 2c.) from the oxygen isotope records to construct our age model. We place our younger age constraint, the transition from marine isotope stage (MIS) 5 to MIS 4 at 13.64±0.35 rmcd. This value, with a conservative estimate for the uncertainty, encompasses the transition to more positive values in both the 1062E and GPC9 δ^{18}O records. We assign this depth an age of 72.0±1.5 ka (Cutler et al., 2003; Lisiecki and Raymo, 2005). For our older age constraint, the change to more negative isotopic values at 20.20±0.40 rmcd is corre-

lated with the transition from MIS 6 to MIS 5 and is assigned an age of 135±1.5 ka (Cheng et al., 2009; Kawamura et al., 2007; Henderson et al., 2001; Thomas et al., 2009; Drysdale et al., 2009). The assigned ages and uncertainties represent the best estimates for these climatic transitions using published ages determined by uranium-series dating of carbonate material such as corals and stalagmites.

Although broadly consistent with the age-models determined on-board the ODP cruise ship (Shipboard Scientific Party, 1998a) and later by Grützner et al. (2002) (using variations in magnetic susceptibility and carbonate content respectively), the δ^{18}O stratigraphy reveals that the transition between MIS 5 and MIS 4 occurs a little deeper in the core (13.64±0.35 rmcd) than suggested by the carbonate content record (12.96 rmcd) (Fig. 2d.). The δ^{18}O transition between MIS 6 and 5 (20.20±0.40 rmcd) is consistent with that suggested by the carbonate record (20.58 rmcd).

5. Palaeomagnetic Methods & Results

All samples were subjected to stepwise alternating-field (AF) demagnetization at applied peak fields of 3, 6, 9, 12, 15, 20, 25, 30, 35, 40, 50, 60, 70, 80, 90 and 100 mT. All measurement and demagnetization steps were performed using a 2G Enterprises DC-SQUID cryogenic magnetometer with an in-line, triaxial, alternating field (AF) demagnetizer in a shielded room at the University of Oxford.

Typical orthogonal demagnetization diagrams of discrete samples from 1062B, D and E are shown in Figure 3. The vast majority of samples displayed a steeply inclined remanent magnetization component which was typ-

ically removed from each sample by peaks fields between 9 and 25 mT. This is most likely an isothermal remanent magnetization (IRM) induced by exposure of the sediment to the magnetized steel core barrel during drilling. This is a common feature of samples from oceanic boreholes and was first noticed in Deep-Sea Drilling Project (DSDP) cores (Ade-Hall and Johnson, 1976).

Principal component analysis (PCA) was used to determine the characteristic remanent magnetization (ChRM). Following removal of the drilling-induced overprint, the majority of samples (80%) display a single, high-stability ChRM. Typically, less than 10% of the total remanence remained after application of the 80 mT peak field. These samples all had ChRMs with maximum angular deviation (MAD) values less than 5°. The high-stability component of magnetization determined suggests that the sediment retains an excellent record of past changes in field direction.

The remaining samples exhibited more complex behaviour; a few samples displayed a randomly oriented low intensity component of remanence that was easily removed by the lowest peak field, 3 mT. This was interpreted as a viscous overprint that was probably acquired during storage. A further group of samples also exhibited a component above 80-90 mT which appeared to have no preferred direction, accounting for 1-5% of the total remanence. At this level, the low signal to noise ratio obscures natural remanence directions.

Samples from intervals during the transitions between polarities often displayed the most complex behaviour accompanied by significantly reduced NRM intensities. In these intervals, the ChRMs were more ambiguous: 17 MAD values exceeded 10° but none of the samples used in later analysis had

MAD values greater than 15°. Only seven samples failed to yield directions fulfilling the above criteria and were subsequently rejected. In general, their ChRMs were not in disagreement with the rest of the record but their MAD values were greater than 15°.

5.1. Palaeomagnetic Directions

All core sections were originally extracted unoriented. Furthermore, the ChRM directions showed progressive trends in declination along core. This was taken as an indication that the cores had been twisted during the drilling process. To examine changes in latitude in the virtual geomagnetic pole we assume that the records conform to a geocentric axial dipole model (GAD) whereby the Earth's field approximates a dipole aligned along the axis of rotation. We oriented all core sections (∼1.5 m length) such that the mean declination outside the excursional interval is oriented towards the geographic North Pole (0°) (Knudsen et al., 2006).

The resulting three records of palaeomagnetic direction (Fig. 4) are remarkably similar and all exhibit a period of excursional behaviour spanning 0.7 m. The average non-excursional inclinations of 46° in 1062B and 43° in both 1062D and 1062E compare well with the expected inclination of 44° for the sites' latitude predicted by the TK03.GAD model (Tauxe and Kent, 2004).

In all three records, the inclination changes rapidly at ∼19 rmcd marking the initiation of the directional excursion (Fig. 4b). A brief peak in positive inclinations is immediately followed by an abrupt change to negative inclinations, reaching a maximum of −55 to −65°. Simultaneously, the declinations swing to 180° (Fig. 4c). This initial transition occurs within 500 years.

Within the excursional interval, 1062B exhibits shallower inclinations than the other two cores. Virtual geomagnetic poles (VGPs) were calculated for each sample using the direction vectors of the respective ChRMs (Fig. 4d). The record shows a rapid transition to fully reversed directions before an equally rapid return to northern latitudes. The limited number of transition VGPs precludes discussion of VGP paths. During non-excursional intervals the variation in the VGP latitude is within that expected of secular variation.

In general, the directions derived from the discrete samples are consistent with earlier continuous split-core measurements (Shipboard Scientific Party, 1998a) although a second, younger, anomalous feature at ∼17 rmcd apparent in the 1062E split-core record is not replicated in the discrete samples measurements (Fig. 4a). The magnetizations of the samples within this interval are indistinguishable from those outside it.

5.2. Core Properties

5.2.1. Isothermal Remanent Magnetization (IRM) Acquisition

To confirm that the geomagnetic field behaviour has been faithfully recorded, it is important to constrain the effects of the mineralogical properties of the sediment cores. Stepwise application of isothermal remanant magnetization may be used to determine the coercivity spectrum of a sample and thereby its constituent magnetic grain mineralogy. After complete demagnetization, a series of 32 representative samples, 16 each from 1062D and 1062E, were subjected to progressive forward-field IRM acquisition using a Molspin Pulse Magnetizer at the University of Oxford. The samples' magnetizations were measured out-of-field between each step using the 2G magnetometer. Subsequently, the samples were subjected to an equivalent series of fields in the

opposite direction (back-field).

The IRM acquisition curves showed that in some cases saturation isothermal remanent magnetization (SIRM) was not achieved by application of an 800 mT field (90-98% saturation). To determine the SIRM, the acqusition curves were modelled using IRMUNMIX (Heslop et al., 2002) assuming a two component mixture of one lower and one higher coercivity component. The model can be used to calculate an estimate for the SIRM. The remanence coercivity (H_{CR}), the 'reverse' field required to reduce a 'forward' saturation remanence to zero, varies between 30 and 40 mT (Fig. 5a). The S-Ratio = -$IRM_{0.3T}$/SIRM was subsequently calculated for all samples. The majority of samples had an S-Ratio greater than 0.85, and no samples measured had an S-Ratio less than 0.7 (Fig. 5b). This indicates that low-coercivity remanence carriers, in this case probably magnetite grains, consistently dominate the magnetic signal. The lack of variation in the H_{CR} values and S-ratios with depth suggests that there has been little change in magnetic grain provenance and mineral composition during the studied time interval. Within the reversed direction interval the S-Ratio value is greater than 0.9 indicating that the contribution of any higher coercivity component is minor.

5.2.2. Magnetic Susceptibility

The magnetic susceptibility of the sediments is dependent upon the concentration, grain-size and mineralogy of the remanence carriers. The IRM acquisition results indicate that the average magnetic mineralogy in the samples does not vary substantially with depth. Therefore variation within the susceptibility record can be used to estimate changes in the size and concentration of the magnetic grains. The low-field magnetic susceptibility of

representative samples was measured using a Geofyzika KLY-2 KappaBridge at Oxford (Fig. 5c). The magnetic susceptibility of the samples shows little variation with depth and is particularly consistent across the excursional interval. Therefore, variation in the intensity of the cores' ChRM is unlikely to be the result of changes in the concentration or grain-size of the remanence carriers.

5.2.3. Grain Size

The ratio of anhysteretic remanence magnetic susceptibility (χ_{ARM}/χ) to low field magnetic susceptibility may be used to investigate first-order variations in grain-size (Banerjee et al., 1981). The magnitude of the ARM is relatively more sensitive to the finer grain-size fraction while low-field magnetic susceptibility (χ) is particularly sensitive to the coarser grain fraction (King et al., 1982). Thus an increase in the proportion of fine to coarse grain magnetite is reflected in shift towards higher χ_{ARM}/χ ratios. An ARM was induced in roughly half of the samples with a 100 mT peak AF field and a 0.1 mT bias field using a DTECH-2000 AF unit which can induce ARMs at Imperial College London. The ARM acquired was subsequently demagnetized at 30 mT.

We observe that the excursional interval is characterized by high values of χ_{ARM}/χ (due to high ARM intensities) representing a higher proportion of fine magnetic grains (Fig. 6a). This feature was also recognized in the same interval by Schwartz et al. (1996) in piston cores from the Blake Outer Ridge. Further study of the piston cores by Schwartz et al. (1997) demonstrated that high values of χ_{ARM}/χ and ARM associated with high S-ratios are most likely indicators of bacterial magnetite content. In such cases, high values

of χ_{ARM}/χ were indicative of the presence of a very fine grained (single domain) magnetite component with high ARM intensities rather than an overall reduction in the size of the clastic magnetite component.

5.3. Relative Palaeointensity Proxies

Sedimentary records have the potential to record variations in the relative palaeointensity of the Earth's field (e.g. Tauxe, 1993). The magnitude of the ChRM is dependent upon a combination of: the magnetic mineralogy of a sample; the concentration of magnetic grains; and the strength of the original field. Although absolute palaeointensity can not be determined, the relative palaeointensity (RPI) variation may be obtained by accounting for the effects of magnetic grain mineralogy and concentration.

We normalize the NRM using the ARM and IRM measurements (Fig. 6c and d). After samples had been subjected to an applied magnetization, they were subsequently demagnetized at 30 mT (Fig. 6b) and the intensities of the remanent NRM, IRMs and ARMs after demagnetization at 30 mT were used to calculate the NRM/ARM and NRM/IRM palaeointensity proxies.

The significant variation in χ_{ARM}/χ suggests that we should approach our interpretation of the relative palaeointensity proxies with a degree of caution (Tauxe, 1993). However, the relative palaeointensity proxies do exhibit a high degree of consistency, both between the individual cores and between the two methods employed to determine relative palaeointensity. Furthermore, the corroboration of the record by three independent cores is evidence that each has, to a reasonable extent, faithfully recorded the intensity of the local palaeomagnetic field.

In general, the relative palaeointensity proxies show a steady decrease in

field intensity from a maximum of 3 or 4 times the average intensity in our record. The field eventually collapses to a significant minimum at 19 rmcd, coinciding with directional excursion. As the field direction returns to normal polarity, the intensity also begins to recover, but this return occurs over an interval of several metres above the directional excursion. Although these general trends are in agreement with palaeointensity stacks (e.g. Ziegler et al., 2011), the potential for sedimentary influences must limit our confidence in any quantification of the relative intensity changes.

6. Constraining Sedimentation Rate

To determine an age and duration for the event in our cores we must first constrain the sedimentation rate. Alone, our oxygen isotope stratigraphy cannot resolve millennial-scale fluctuations in sedimentation rate between the two age-constrained stratigraphic bounds. However, unlike records of the Blake excursion from other marine cores, we do not have to assume an average sedimentation rate within a broad interval in the stratigraphy. Instead, using the excess ^{230}Th approach (Francois et al., 2004; Henderson and Anderson, 2003) we can reconstruct sedimentation rate variations relative to the average sedimentation rate between the age-constrained bounds. Following the approach of Knudsen et al. (2007), we determine an accurate age and duration for the Blake excursion in our record and also provide precise uncertainties. Thus, the chronology we employ to estimate the age and duration of the excursion does not suffer from the limited resolution that has hindered many earlier attempts to estimate the ages and durations of short duration events in the past.

^{230}Th is produced in the water column by the decay of dissolved ^{234}U. Unlike ^{234}U, ^{230}Th is highly insoluble. As a result, it is rapidly adsorbed onto the surfaces of sinking particles and transported to the underlying sediment: a process known as 'scavenging' (Bacon and Anderson, 1982). This component of the ^{230}Th in the sediment is termed 'excess' thorium ($^{230}\mathrm{Th}_{xs}$) as it is not supported by any corresponding uranium component.

The flux of $^{230}\mathrm{Th}_{xs}$ to the seafloor is dependent only upon the depth of the overlying water column and the concentration of ^{234}U in seawater, both of which are unlikely to have varied considerably over the last several hundred thousand years (Henderson, 2002). Modelling the variability of the flux of $^{230}\mathrm{Th}_{xs}$ into the sediment via scavenging using an ocean general circulation model (Henderson et al., 1999) indicates that the flux at the location of Site 1062 is likely to have been relatively constant and equivalent to its production rate in the water column. The concentration of the $^{230}\mathrm{Th}_{xs}$ in the sediment is therefore dependent upon the sedimentation rate. By measuring the concentration of $^{230}\mathrm{Th}_{xs}$ in the sediment we can determine relative variations in total sediment flux. We assume a simple reciprocal relationship whereby a doubling of the sedimentation rate would halve the measured $^{230}\mathrm{Th}_{xs}$ concentration.

The relatively high average sedimentation rate between the age-constrained bounds ($\sim$10 cm kyr^{-1}) suggests that there is some lateral input of material to the site. Our method assumes that the degree of syndepositional lateral redistribution or 'focussing' of sediment remains constant at the site throughout this interval. The Blake Outer Ridge and surrounding sediments owe their existence to the influx and deposition of terrigenous sediments car-

ried from the north by the deep, geostrophic Western Boundary Undercurrent (WBUC) (Heezen et al., 1966). The Gulf Stream flows rapidly northwards along the western margin of the Blake Plateau separating the ridge from the potential sediment source of the eastern margin of the continent (Heezen et al., 1966). ODP Site 1062, south of the Blake Outer Ridge and east of the Blake Plateau, is therefore in a relatively 'sheltered' location. The lack of variation in magnetic grain mineral composition and concentration throughout our studied interval (Fig. 5) suggests that the sedimentary environment remained relatively constant during our sampled interval.

Scavenging is not, however, the only source of ^{230}Th into the sediment. To determine the contribution of $^{230}\mathrm{Th}_{xs}$ to the total ^{230}Th content of the sediment, contributions from ^{230}Th supported by detrital U ($^{230}\mathrm{Th}_{det}$) and ^{230}Th ingrown from authigenic U ($^{230}\mathrm{Th}_{auth}$) must be subtracted from the total measured activity of ^{230}Th, such that:

$$^{230}\mathrm{Th}_{xs} = ^{230}\mathrm{Th}_{meas} - ^{230}\mathrm{Th}_{det} - ^{230}\mathrm{Th}_{auth} \quad (1)$$

We conducted ^{230}Th measurements on 18 samples spanning the MIS 5 interval of core 1062E. For each sample measured, 0.1 g of dry sediment was dissolved following the method outlined in Thomas et al. (2007). For two of the samples, a further 0.1 g of sediment was dissolved independently to test repeatability. U and Th were then chemically separated from the solution via anion chromatography (Robinson et al., 2004). The samples were spiked with a mixed ^{229}Th and ^{236}U spike and concentrations of the isotopes ^{234}U and ^{238}U were measured statically and ^{230}Th and ^{232}Th were subsequently measured dynamically, on a Nu Instruments ICP-MS at the Department

of Earth Sciences, University of Oxford (Mason and Henderson, 2010) (see Supplementary Material).

We calculate the detrital component of the total measured ^{238}U and use this to determine the detrital input of ^{230}Th. $^{238}U_{det}$ is calculated by assuming that all of the ^{232}Th in the sample is of detrital origin and using an appropriate value for $(^{238}U/^{232}Th)_{det}$.

$$^{230}Th_{det} = \left(\frac{^{230}Th}{^{238}U}\right)_{det} \times ^{238}U_{det} = \left(\frac{^{230}Th}{^{238}U}\right)_{det} \times \left[\left(\frac{^{238}U}{^{232}Th}\right)_{det} \times ^{232}Th\right] \quad (2)$$

To estimate $(^{238}U/^{232}Th)_{det}$, we identified the samples unlikely to have a thorium contribution from the decay of authigenic uranium. The distribution of measured $^{238}U/^{232}Th$ ratios from our samples includes one group with consistently low values averaging 0.53 ± 0.09 (Fig. 7). The remaining samples have a range of values greater than 0.7. We interpret the first group to represent those samples with limited or no authigenic uranium component, the higher uranium group are therefore identified as those that have had varying contributions of authigenic uranium in addition to the detrital input. We therefore use a value of 0.53 ± 0.09 for $(^{238}U/^{232}Th)_{det}$, consistent with the range typical for Atlantic sediments (=0.6±0.1 Henderson and Anderson, 2003).

If ^{230}Th were in secular equilibrium with ^{238}U in marine detrital material, $(^{230}Th/^{238}U)_{det}$ would equal 1, however, $(^{230}Th/^{238}U)_{det}$ may be less than 1 due to alpha recoil from smaller particles (Osmond and Ivanovich, 1992). We estimate the deviation of the system from equilibrium by averaging the measured $^{234}U/^{238}U$ ratios from samples thought to be free of authigenic uranium ($= 0.98 \pm 0.02$). The $(^{230}Th/^{238}U)_{det}$ ratio is likely to be lower

than this due to further alpha recoil during the decay of ^{234}U to ^{230}Th. We therefore estimate $(^{230}\mathrm{Th}/^{238}\mathrm{U})_{det}$ by doubling the deviation of the measured $^{234}\mathrm{U}/^{238}\mathrm{U}$ average from secular equilibrium to give a $(^{230}\mathrm{Th}/^{238}\mathrm{U})_{det}$ ratio of 0.96 ± 0.04.

Any remaining ^{238}U not accounted for by lithogenic material is assumed to be of authigenic origin. The component of ^{230}Th produced by the decay of authigenic ^{238}U in each sample ($^{230}\mathrm{Th}_{auth}$) is given by (Henderson and Anderson, 2003):

$$^{230}\mathrm{Th}_{auth} = \left(^{238}\mathrm{U}_{tot} - ^{238}\mathrm{U}_{det}\right) \times \left[\left(1 - e^{-\lambda_{230}t}\right) + \frac{\lambda_{230}}{\lambda_{230} - \lambda_{234}}\left(\frac{^{234}\mathrm{U}}{^{238}\mathrm{U}_{init}} - 1\right)\left(e^{-\lambda_{234}t} - e^{-\lambda_{230}t}\right)\right] \quad (3)$$

Where λ is the decay constant in yr^{-1}, t is the age (derived from the δ^{18}O stratigraphy), and $(^{234}\mathrm{U}/^{238}\mathrm{U})_{init}$ is the initial ^{234}U to ^{238}U ratio in seawater (=1.146) (e.g. Robinson et al., 2004). The current $^{230}\mathrm{Th}_{xs}$ activity may then be determined using Equation 1. The initial $^{230}\mathrm{Th}_{xs}$ concentration was then calculated by correcting for its own decay:

$$^{230}\mathrm{Th}^{\circ}_{xs} = ^{230}\mathrm{Th}_{xs} e^{\lambda_{230}t} \quad (4)$$

The sedimentation rate, $\mathrm{F}_{(n)}$ (in cm kyr^{-1}) for each sample interval was then calculated using the following expression:

$$\mathrm{F}_n = \mathrm{F}_a \times \frac{\overline{\mathrm{Th}}}{\mathrm{Th}_n} \quad (5)$$

Where Th_n is the concentration of $^{230}\mathrm{Th}_{xs}$ in sample n; F_a is the average sedimentation rate in cm kyr^{-1} between the two boundaries of known age

and $\overline{\mathrm{Th}}$ is the weighted average concentration of $^{230}\mathrm{Th}_{xs}$ between the boundaries. This assumes a simple reciprocal relationship whereby the variation in the initial concentration of initial $^{230}\mathrm{Th}_{xs}$ about the weighted average initial $^{230}\mathrm{Th}_{xs}$ is proportional to the variation of the sedimentation rate about the average between the boundaries.

The average sedimentation rate between the boundaries (72–135 ka) is 10.4 cm kyr^{-1}. Our thorium data indicate that the standard deviation of the rate is only 1.6 cm kyr^{-1} and therefore that the sedimentation rate is rather constant during MIS 5, despite climatic changes. The constancy of sedimentation rate allows us to confidently calculate a duration for the Blake excursion from our new high-resolution record and to assess the uncertainty on this duration. Using the dry bulk density measured on-board ship of 0.74 g cm^{-3} (Shipboard Scientific Party, 1998a) and employing the equations given by Francois et al. (2004), we calculate a focusing factor (Ψ) of 4.2. Using a third age constraint at the end of MIS 5e, we investigated to what extent the focussing remained constant throughout MIS 5 (available as supplementary material). Our estimates suggest that the focussing factor may vary by up to $\sim$5%. This source of uncertainty is included in our uncertainty for the interval duration.

7. Duration and Age of the Blake Excursion at Site 1062

For the sake of comparison with previous studies of excursions, we use a conventional co-latitude VGP cut-off whereby the duration of an excursion is the period of time the VGP spends more than 45° from the geographic north pole (assumed to be equivalent to the long-term time-averaged VGP

position) (Merrill and McFadden, 1994). Following this definition, the Blake excursion spans 0.7 m (the interval 18.8–19.5 rmcd). If we instead examine the deviation of VGPs away from 'normal' secular variation using the adaptive approach of Vandamme (1994), we obtain a VGP cut-off value from our data of 27° co-latitude. Due to the rapid change between reversal states, the use of this alternative cut-off value defines a very similar excursion interval. Assuming a constant sedimentation rate, between the boundaries, of 10.4 cm kyr^{-1} the duration of the directional excursional interval would be 6.7 kyr. Using the refined, thorium-corrected sedimentation rates, the duration of the excursional interval is 6.5±1.3 kyr, with the event occurring between 128.5±4.0 ka and 122.0±3.9 ka (note that while the ages have a larger uncertainty, they co-vary, such that the duration has a relatively low uncertainty). To precisely constrain the uncertainties on the duration and age of the excursion, we use a Monte-Carlo method in which the input isotopic data are assigned normal distribution probability density functions and the age and depths of the age-constrained boundaries are varied randomly between maxima and minima. The uncertainty on the duration estimate is principally controlled by potential variation in focussing and the uncertainties assigned to the age and depths of the boundaries.

Our chronology for the Site 1062 cores is in good agreement with the most precise radiometric age for the start of the excursion (132.8±1.3 ka) (Ménabréaz et al., 2010). However, the stratigraphic relationship between MIS 5e and the excursional event provides an easier way to compare our record with previously published marine core and Loess records because previous records have assumed different chronologies for the oxygen isotope record. In our

Site 1062 record, the Blake excursion is almost exactly coeval with MIS 5e and the changes in inclination span the entire MIS 5e interval. Mediterranean cores at a similar latitude show that the local directional excursion occurred towards the end of the MIS 5e (Tric et al., 1991; Tucholka et al., 1987), and Arctic records similarly show the excursion coinciding with MIS 5e (Nowaczyk et al., 1994).

If 'lock-in' has occurred at depth below the sediment surface, the age of the measured magnetic signal would be younger than the sediment in which it was recorded and thus the stratigraphic chronology would overestimate the age of the excursion. By studying a core with a relatively high sedimentation rate, $\sim$10 cm kyr^{-1}, we reduce the likelihood of there being a significant 'lock-in' depth (Roberts and Winklhofer, 2004). The sharp transitions between polarity states in the Site 1062 record suggest that 'lock-in' of the magnetic signal occurs across a limited depth range throughout the record of the excursion. The sedimentation rate is also relatively constant. Thus, even if there is a 'lock-in' depth, it is likely to be constant, such that while the age of the excursion may be less, the calculated duration of the excursion is unlikely to change significantly.

8. Discussion

Our new data provides the highest resolution record yet analysed of the Blake geomagnetic excursion. The agreement between the 3 cores indicates that the Site 1062 sediments are excellent recorders of the palaeomagnetic field, yielding high-quality palaeomagnetic vectors with low MAD values.

8.1. Geometry of the Excursional Field

The cores from Site 1062 record a fully reversed field, consistent with some previously obtained records of the Blake excursion (e.g. Fang et al., 1997; Zhu et al., 1994). However, unlike the records of the Blake excursion from the Mediterranean (Tric et al., 1991) and Chinese loess (Fang et al., 1997; Zhu et al., 1994), the cores from Site 1062 do not record multiple reversed intervals separated by normal polarity intervals.

Although cores that record only a single reversed interval have generally been attributed to the filtering of the magnetic signal by low sedimentation rate cores (Tucholka et al., 1987; Tric et al., 1991), the high sedimentation rate ($\sim$10 cm kyr^{-1}) of the Site 1062 cores, the high resolution of our new record, and the recording of rapid polarity transitions imply that the geomagnetic signal from Site 1062 is well-resolved. Furthermore, the relatively constant sedimentation rate and long duration of the excursion suggest that a hiatus in the Site 1062 record, which could encompass a normal polarity interval during the excursion, is unlikely and was similarly not found in previous age models (Fig. 2d) (Grützner et al., 2002).

Our new record therefore calls the global existence of multiple reversed intervals into question and suggests that such behaviour should not be considered as characteristic of the Blake excursion.

8.2. Duration of Geomagnetic Excursions

Our record from Site 1062 indicates that the geomagnetic field deviated from directions that might be expected during 'normal' secular variation for 6.5$\pm$1.3 kyr. This duration is within previous estimates for the duration of the Blake excursion (3.5–8.6 kyr) (Tric et al., 1991; Zhu et al., 1994; Fang

et al., 1997) but is robust due to the high sedimentation rate and $^{230}Th_{xs}$ constrained chronology. Although the duration of the Blake excursion's expression in the directional record may vary between locations, the internal process that caused the excursion must therefore have had a relatively 'long' minimum duration of ∼6 kyr to create the signal found in our record.

The duration of the Blake excursion is therefore significantly longer than that determined for the Laschamp excursion (∼2 kyr) (Laj et al., 2000, 2006) at a number of global sites, including the North Atlantic, and is comparable with the duration of the Iceland Basin excursion (6.8±0.5 kyr) (Knudsen et al., 2007) recorded at Site 1063 in the North Atlantic from the same ODP leg. Directional excursions therefore occupy a broad range of durations and can feature a reversed polarity field state for more than ∼3 kyr without this resulting in a full polarity reversal.

8.3. Rapid Transitions

Unlike previous records of the Blake excursion (Tric et al., 1991; Tucholka et al., 1987), Site 1062 fails to record the transitional field in any detail despite a relatively high sedimentation rate (∼10 cm kyr^{-1}). Furthermore, the Site 1062 record of the Blake excursion implies rapid and complete reversals in field direction within periods of less than 500 years corresponding to a VGP transition rate of $\sim 180^{\circ}$ kyr^{-1}. The rapid transition rate in this record suggests that our long duration for the Blake excursion is compatible with much shorter duration estimates for other excursions such as the Laschamp whereby the difference in duration of the event arises as a result of the length of time the field remains in a fully reversed state rather than differences in the durations of the transitions. Furthemore, this rate of change is simi-

641 lar to that observed for the IBE transitions in the North Atlantic (Knudsen
642 et al., 2007) and notably faster than that during reversals. During a reversal,
643 the single polarity transition takes ∼5 kyr, corresponding to a rate of only
644 18° kyr^{-1} (Clement, 2004). The rapidity of the transitions observed in high
645 resolution records of excursions is a particularly striking feature, providing
646 clues about the mechanism that generates field change (Fig. 9). Any mech-
647 anism or mechanisms to explain excursions and reversals must therefore be
648 able to account for the significant difference in transition rate between the
649 two.

650 *8.4. Stability of the Excursional Field*

651 Recent simulations of field reversals, using a time-varying observational
652 model of the geomagnetic field for the last 7000 years (Korte, 2005), assume a
653 decreased dipole strength to be the cause of transitional fields (Brown et al.,
654 2007; Valet and Plenier, 2008). Excursions are simulated in these models by
655 setting the strength of the dipole to a reduced value for a set time interval.
656 The axial dipole field strength must be decreased significantly (to around
657 20%) before large excursional events are observed in the simulations (Brown
658 et al., 2007). Such a decrease in intensity is observed in our record for the
659 Blake, and similarly during other polarity transitions (Ziegler et al., 2011),
660 whereby the relative palaeointensity decreases over a significantly longer du-
661 ration interval before the directional excursion is recorded, and its subsequent
662 increase in strength occurs after the field direction has returned to its intial
663 polarity. However, it is difficult to imagine how a time-varying non-dipole
664 field could maintain fully reversed directions for such a long duration as that
665 found for the Blake excursion in our record (6 kyr+).

Valet and Plenier (2008) simulate excursions in a similar model by decreasing the axial dipole strength to zero and then increasing it back to its initial state - a situation equivalent to that of a full reversal. This approach explores therefore the possibility that a geomagnetic excursion could represent an 'aborted' polarity interval (Valet et al., 2008). However, they could only simulate directional records with VGPs in high southerly latitudes by adding a short interval of a weakly reversed dipole field before the return of the field to its initial state. This suggests that an extended duration interval with fully reversed directions, such as that found in our Blake record, must represent a short period when there is a weak, reversed polarity dipole field. Our record does not, however, document an increase in field intensity within the directional excursion, which implies that the strength of the dipole must still be minimal and that this interval still represents an unstable field state.

9. Conclusions

- Combining a δ^{18}O stratigraphy and the ^{230}Th excess method, our new high-resolution palaeomagnetic record of the Blake excursion at ODP Site 1062 indicates that the geomagnetic field deviated from directions expected during 'normal' secular variation for 6.5±1.3 kyr between 129 and 122 ka. This is within the range of previous estimates of the duration of the Blake excursion (3.5–8.6 kyr) at other sites, but previous estimates have generally relied on average sedimentation rates across broad depth intervals. '

- Our relatively long duration for the Blake excursion at Site 1062 is evidence that excursions do not necessarily have short durations (i.e.

690 < 3 kyr) but instead occupy a continuous range of durations. Further-
691 more, the maintenance of fully reversed directions for a long duration
692 implies the presence of a weakly reversed dipole during the excursion.

693 • However, despite the length of the Blake excursion, the record of the
694 event at Site 1062 is characterized by rapid polarity transitions (< 500
695 years) that are significantly faster than those observed during reversals.

696 • The ^{230}Th-excess method shows great promise in constraining the du-
697 ration of short (kyr) events for other records where sedimentation rates
698 may potentially vary more significantly than at Site 1062.

699 • To understand further the true nature of the global geomagnetic field
700 during the Blake excursion, high quality records are required from a
701 number of locations from across the globe particularly from the south-
702 ern hemisphere (Roberts, 2008). Our new record provides the first
703 steps toward a global dataset of high-quality palaeomagnetic data with
704 precise chronological control for the Blake excursion.

705 Acknowledgements

706 Samples were provided by the Ocean Drilling Program (ODP) and we
707 thank the Bremen Core Repository (BCR) team for their assistance. The
708 ARM acquisitions were carried out with the assistance of Adrian Muxworthy
709 at Imperial College London. This work was supported by a NERC stu-
710 dentship to Mark Bourne and by NERC grants NER/T/S/2003/00041 and
711 NE/G001391/1.

Location	Medium*	Site	Lat.	Long.	Dating	Sed. Rate (cm kyr^{-1})	Duration (kyr)	Age / MIS (ka)	Principal Reference
New Mexico	B	Laguna Basalt	35.1	252.3	K/Ar	-	-	128±33	1
Hawaii	B	Hawaii	19.7	155.1	Ar/Ar	-	-	132±32	2
NE China	B	Jilin Province	42.1	128.0	Ar/Ar	-	-	123±7	3
Tahiti	RC	IODP310 M0005	17.8	-149.6	U/Th	-	-	133±1/5e	4
Xining, W China	L	Xining	36.6	101.8	TL*	9.8	5.3	5d	5
W. Plateau, China	L	Lanzhou	36.0	103.8	TL*	2	5.5	5e	6
Blake Ridge, Caribbean	MS	RC10-49	16.6	-79.5	d18O	3.4	5	-	7
Blake Ridge, Caribbean	MS	A179-4	16.6	-74.8	d18O	2.4	7	5e	7
E. Mediterranean	MS	MD84641	33.0	31.4	d18O	2.3	3.5	-	8
W. Mediterranean	MS	KET8004	39.7	12.4	d18O	6.4	8.6	5e/5d	8
W. Mediterranean	MS	KET8022	40.6	10.3	d18O	5.5	6.4	Spans 5e	8
E. Mediterranean	MS	MD84640	33.1	-32.9	d18O	8	4	end of 5e	8
E. Mediterranean	MS	MD84627	32.2	32.3	d18O	10.5	4.5	end of 5e	8,9
W. Mediterranean	MS	DED8707	39.7	-12.4	d18O	10.5	4	5e	9
Yermack Plateau, Arctic	MS	PS 1533-3 SL	82.0	15.2	d18O	2	10	Start 5e	10
Yermack Plateau, Arctic	MS	PS 2212-3 KAL	82.1	15.9	d18O	6	10	Start 5e	10
Amazon Fan	MS	942A/946A	5.7	-49.1	d18O	100	-	5e	11

Table 1: Age and duration estimates for the Blake Excursion. *B: Basalt, L: Loess, MS: Marine sediment, TL: Thermoluminescence dating and correlation using magnetic susceptibility. RC: Reef carbonate. References: (1) Champion et al. (1988), (2) Holt and Kirschvink (1996), (3) Zhu et al. (2000), (4) Ménabréaz et al. (2010) - note that date is the start of excursion, (5) Zhu et al. (1994), (6) Fang et al. (1997), (7) Smith and Foster (1969), (8) Tucholka et al. (1987), (9) Tric et al. (1991), (10) Nowaczyk et al. (1994), (11) Cisowski and Hall (1997).

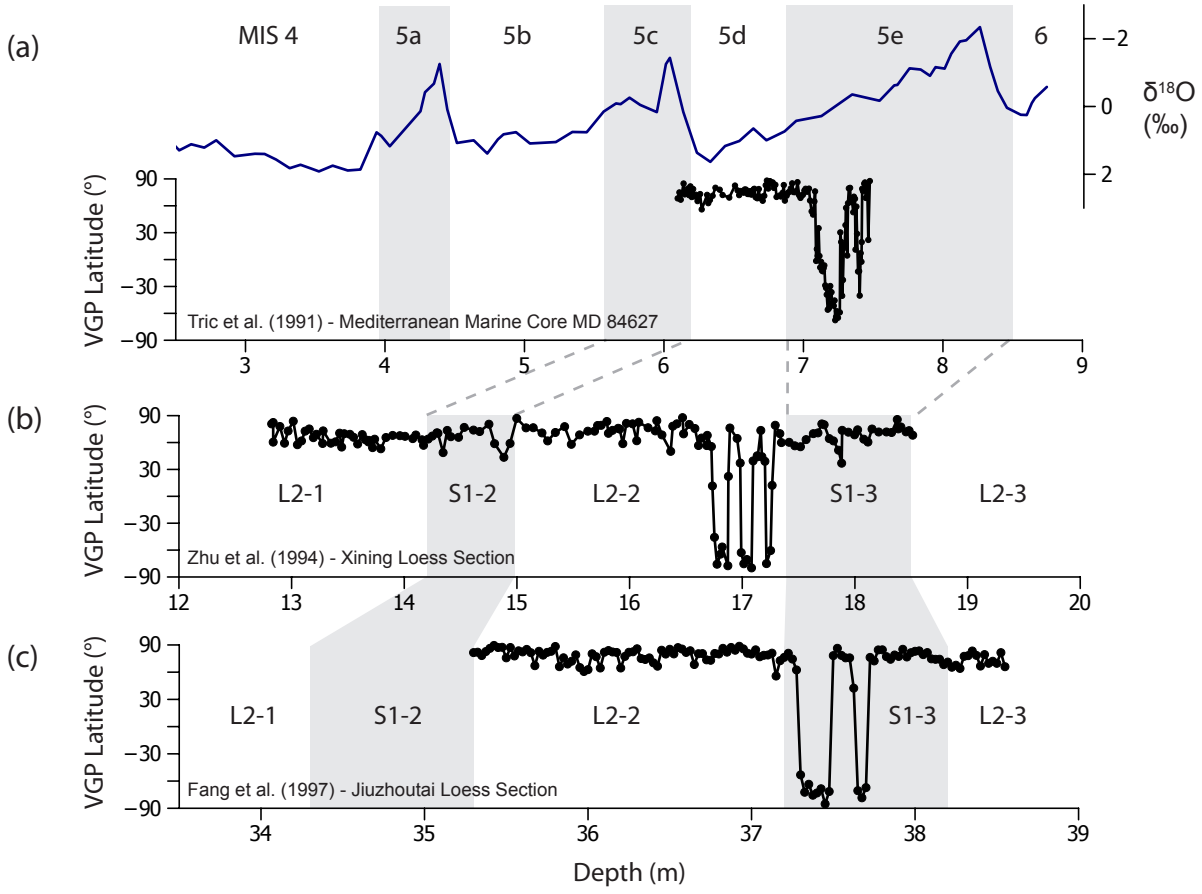

Figure 1: Three of the highest resolution records of the Blake excursion from the literature. (a) δ^{18}O stratigraphy for Mediterranean core MD 84627 with Marine Isotope Stages (MIS) identified, and below, the VGP latitude curve from the same core (Tric et al., 1991). (b) VGP latitude record from Xining Loess section, with palaeosol (grey bars) and loess stratigraphy correlated to MIS (dashed lines) (Zhu et al., 1994). (c) VGP latitude record for Jiuzhoutai Loess section and section stratigraphy (Fang et al., 1997).

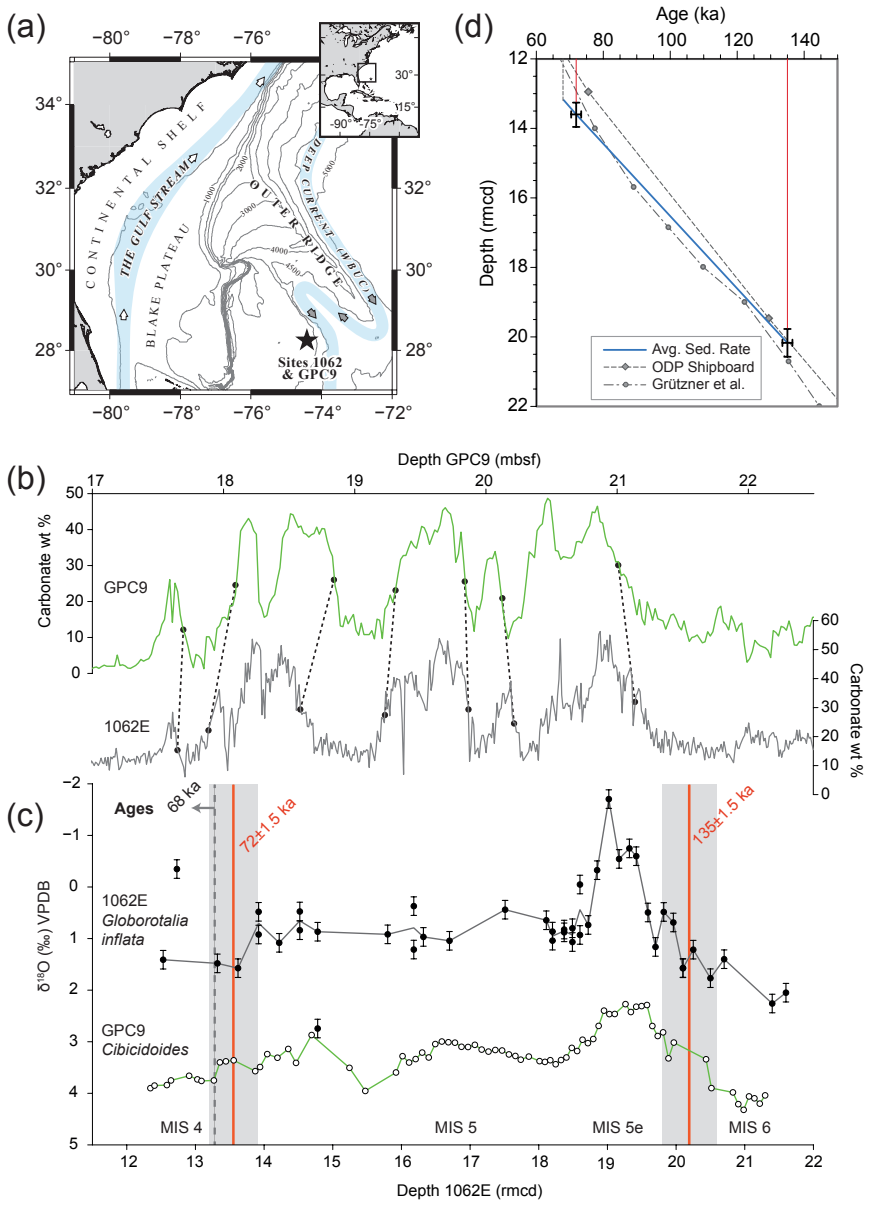

Figure 2: (a) Location of Site 1062 and GPC9 (WBUC - Western Boundary Undercurrent). Bathymetry data taken from 'The GEBCO One Minute Grid, version 2.0, http://www.gebco.net'. (b) Carbonate records from GPC9 (Keigwin et al., 1994) and 1062E (Giosan et al., 2001). Correlated features used as tie-points marked by grey dashed lines. 1062E Depth in 'rmcd' (see text) equivalent to metres below seafloor (mbsf). (c) 1062E and GPC9 δ^{18}O records on Core 1062E depth scale (rmcd). δ^{18}O measured with respect to the Vienna PeeDee Belemnite carbonate standard in delta notation (‰). Age constraints in the δ^{18}O stratigraphy for the MIS 6/5 & MIS 5a/4 transitions are marked in red with assumed depth uncertainties shown by the grey bars. Last appearance of *Globorotalia tumida flexuosa* (68 ka) marked with grey arrow. (d) Age-depth plot of core 1062E. Age constraints used in this study are marked in red. Solid blue line assumes average sedimentation between selected age constraints, dashed grey lines show previous age models (Shipboard Scientific Party, 1998a; Grützner et al., 2002).

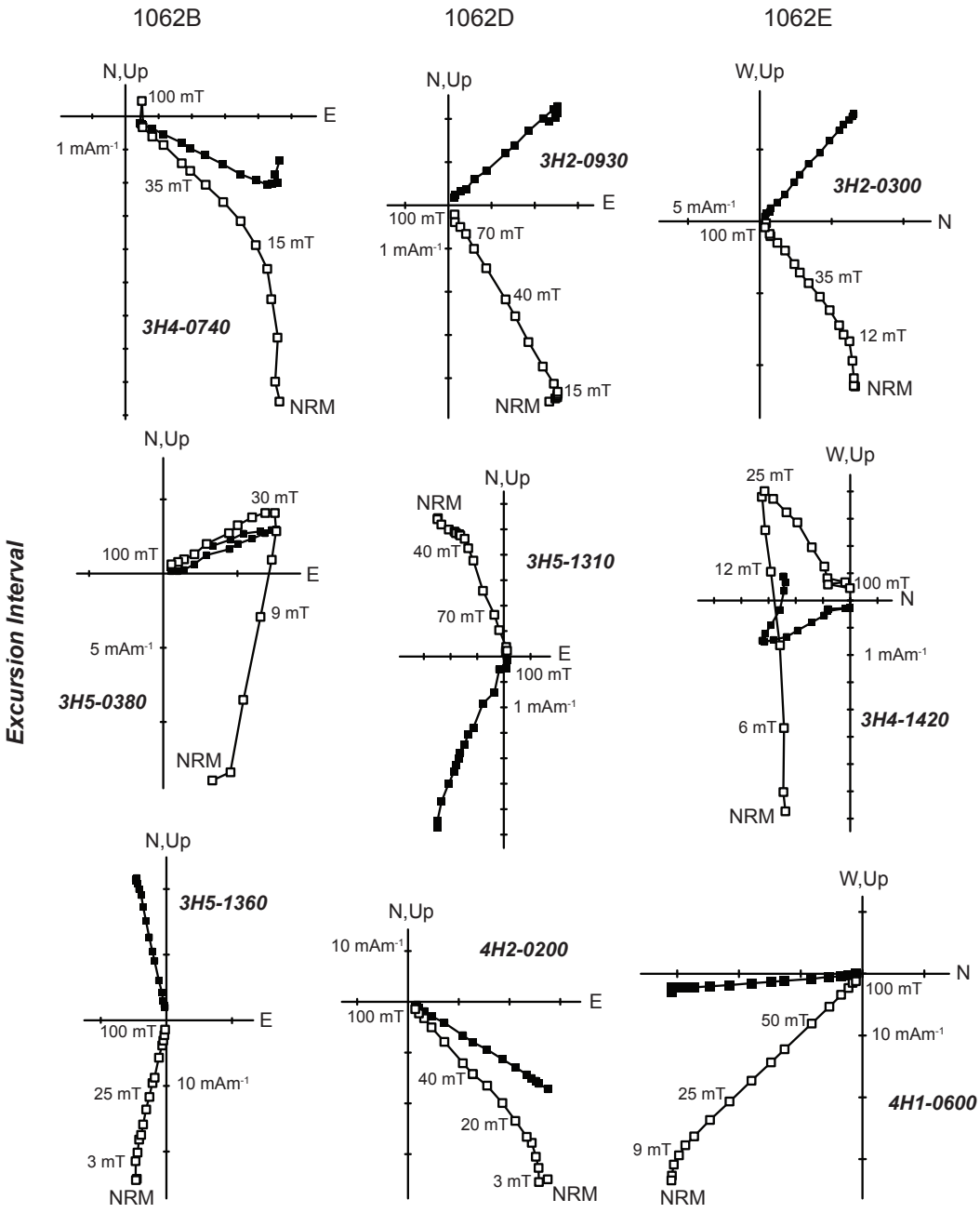

Figure 3: Typical orthogonal demagnetization plots for samples from Cores 1062B, D and E. The top and bottom rows are representative of samples younger and older than the excursional interval (middle row) respectively. Sample declinations are unoriented. Magnetization of sample in milli-Amps per metre (mAm^{-1}). Applied alternating-field (AF) demagnetization field strength in milli-Tesla (mT). Open (solid) squares represent the projection of the magnetic vector onto the vertical (horizontal) plane.

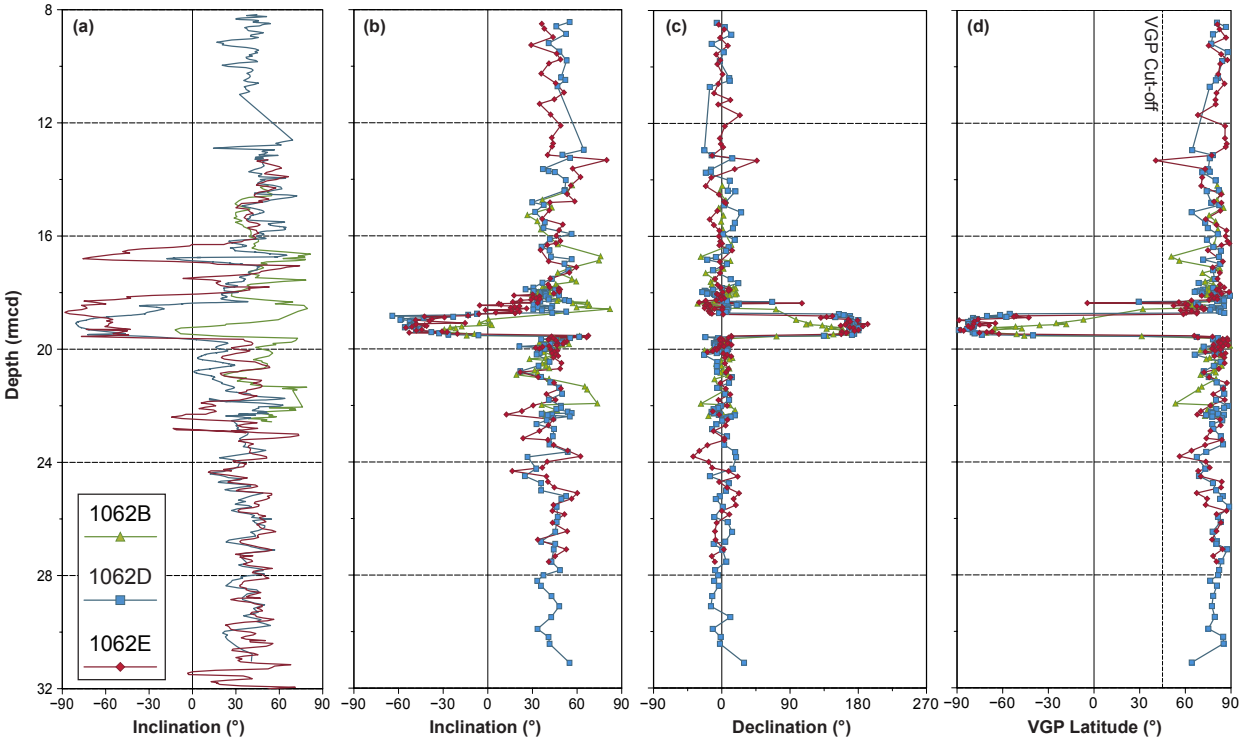

Figure 4: (a) Inclinations of the ChRMs of samples from cores 1062B,D and E against depth (rmcd) measured from split-cores on-board ship (Shipboard Scientific Party, 1998a), and (b) from discrete samples (this study). (c) Corrected declinations of discrete samples. (d) Calculated latitude of the virtual geomagnetic poles (VGPs) for all samples. VGP cut-off co-latitude used to define limits of directional excursion marked by dashed line at 45°.

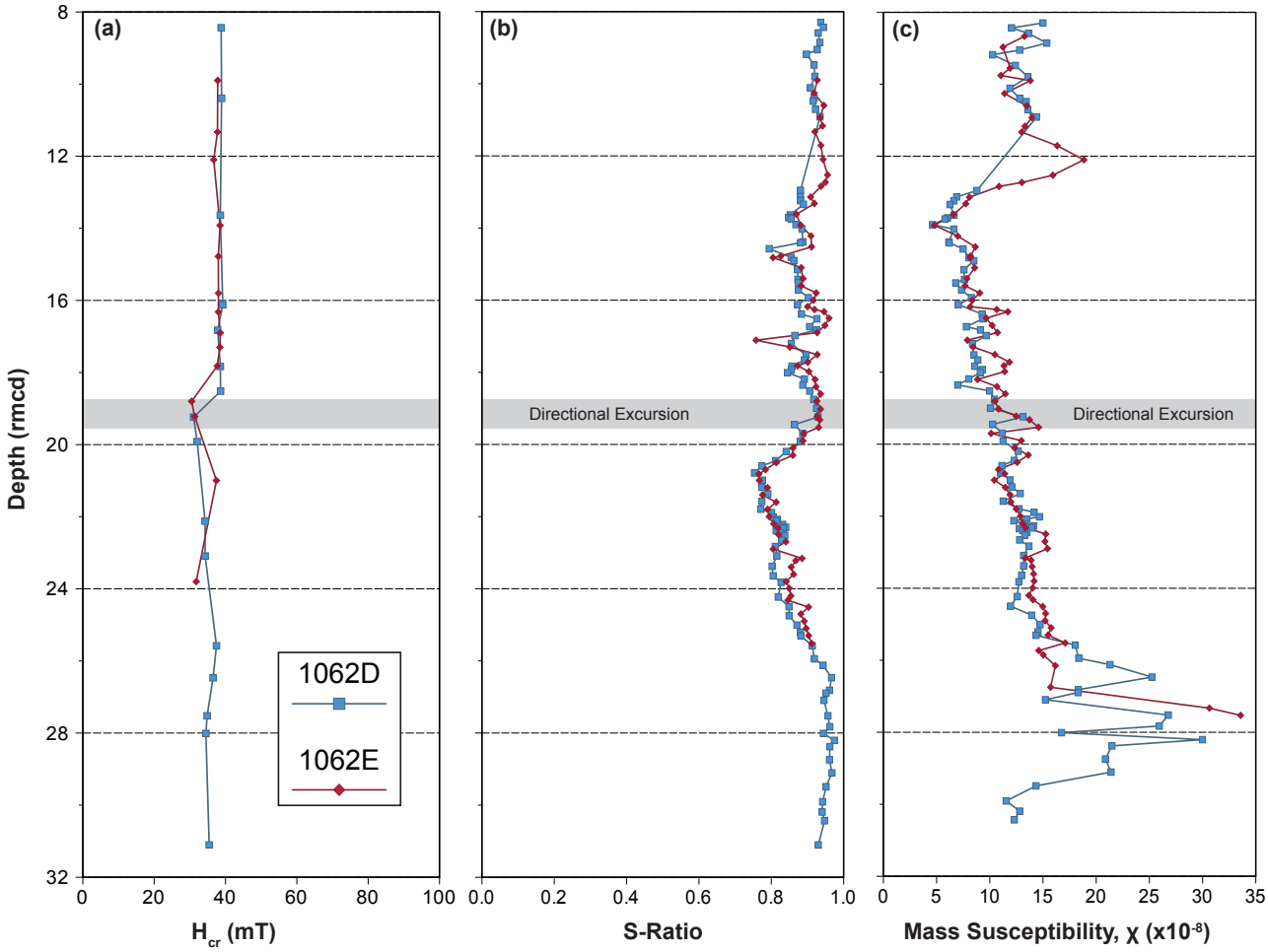

Figure 5: (a) Remanence coercivity (H_{cr} of measured samples in milli-Tesla (mT) from cores 1062D and E against depth (rmcd). (b) S-Ratio (dimensionless - S-Ratio = -$IRM_{0.3T}/IRM_{0.8T}$). (c) Mass specific magnetic susceptibility (χ). (10^{-8} m^3 kg^{-1}). Directional excursional interval highlighted by grey-shaded bar defined as in Figure 4.

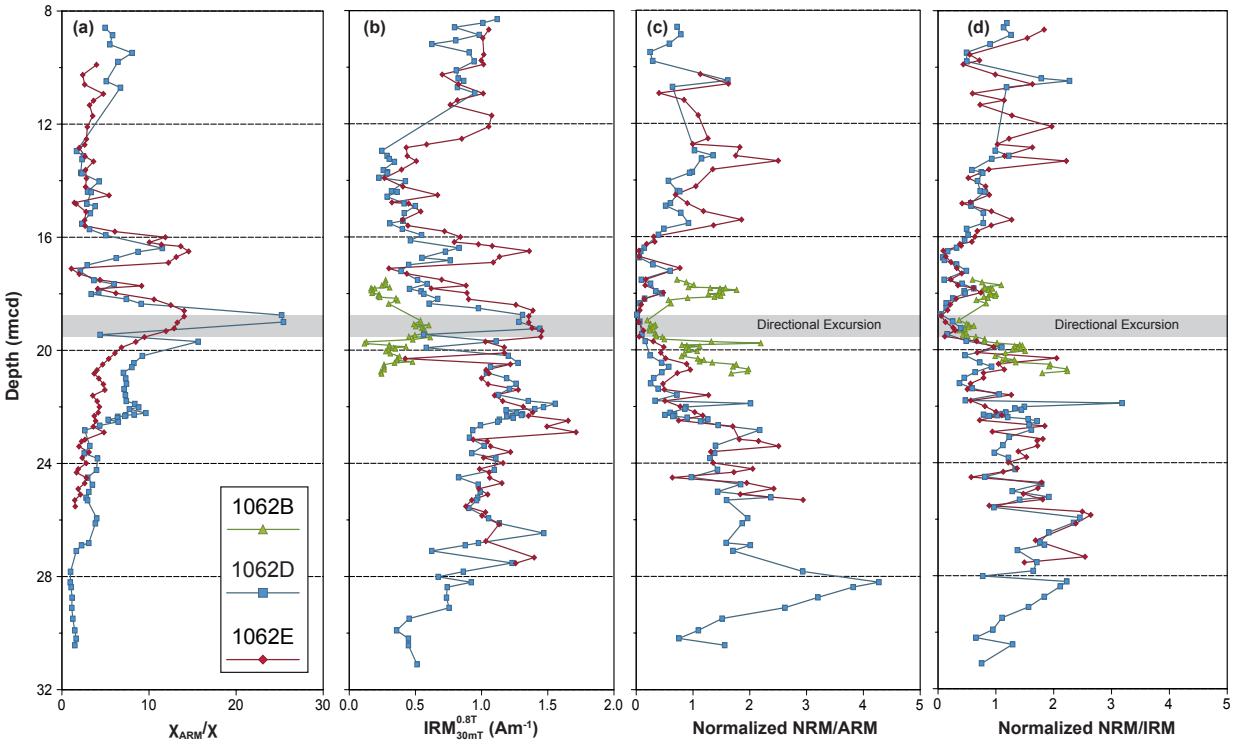

Figure 6: (a) Anhysteretic magnetic susceptibility divided by the measured magnetic susceptibility (χ_{ARM}/χ) for samples from cores 1062D and E. (b) Intensity of applied isothermal remanent magnetization (at 0.8 T) following AF demagnetization at a peak-field of 30 mT. Relative palaeointensity records (c) and (d) for 1062B, D and E derived by dividing the natural remanent magnetizations by the measured anhysteretic and isothermal magnetizations respectively (normalized such that the average values for the records are equal to 1). Directional excursional interval highlighted by grey-shaded bar defined as in Figure 4.

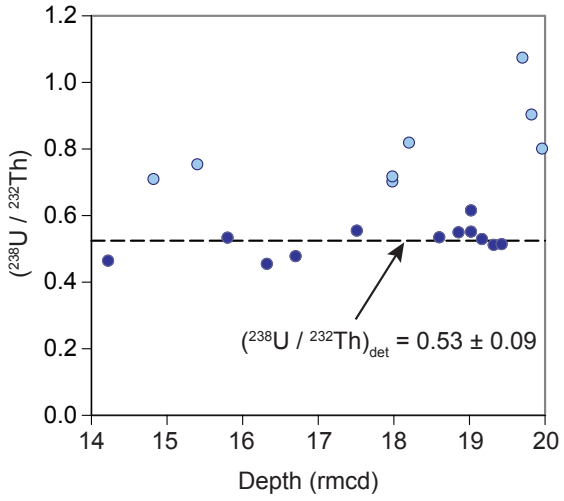

Figure 7: The distribution of measured $^{238}\mathrm{U}/^{232}\mathrm{Th}$ ratios from our samples. One group of samples has consistent low values averaging 0.53 ± 0.09 (dark blue circles), interpreted as the value for $(^{238}\mathrm{U}/^{232}\mathrm{Th})_{det}$. The remaining, higher uranium group (light blue circles) are identified as those that have had varying contributions of authigenic uranium in addition to the detrital $^{238}\mathrm{U}$.

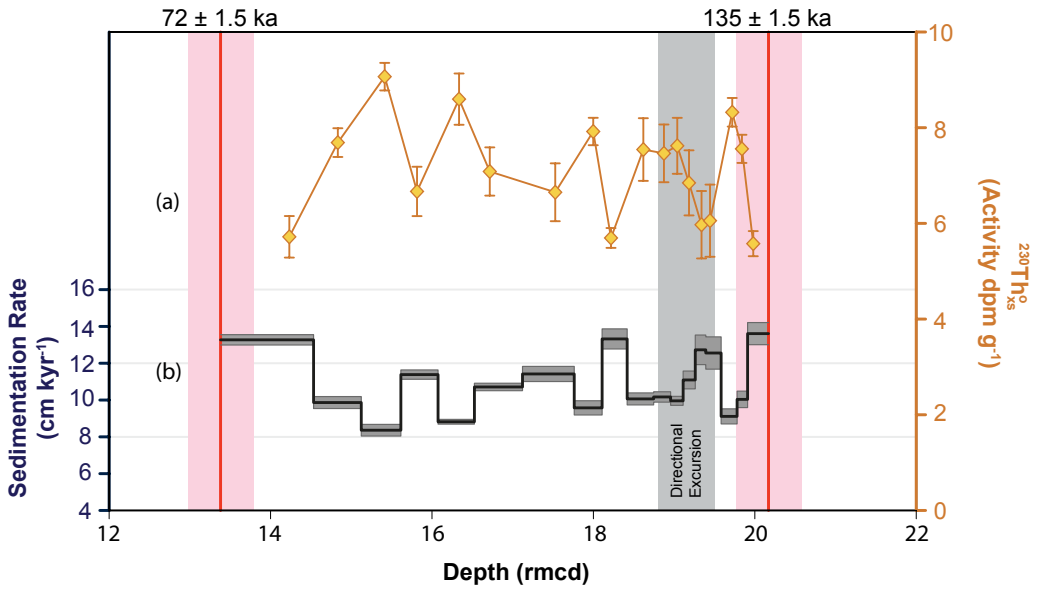

Figure 8: (a) Calculated $^{230}\mathrm{Th}^{\circ}_{xs}$ (orange diamonds) in decays per minute per gram (dpm g^{-1}) with 2σ uncertainty in core 1062E (rmcd). (b) $^{230}\mathrm{Th}^{\circ}_{xs}$-normalized sedimentation rate (solid line) between the two age constraints marked in red (72 and 135 ka in cm kyr^{-1}) with depth uncertainty envelopes in pink. Grey envelope indicates 2σ uncertainty on sedimentation rate.

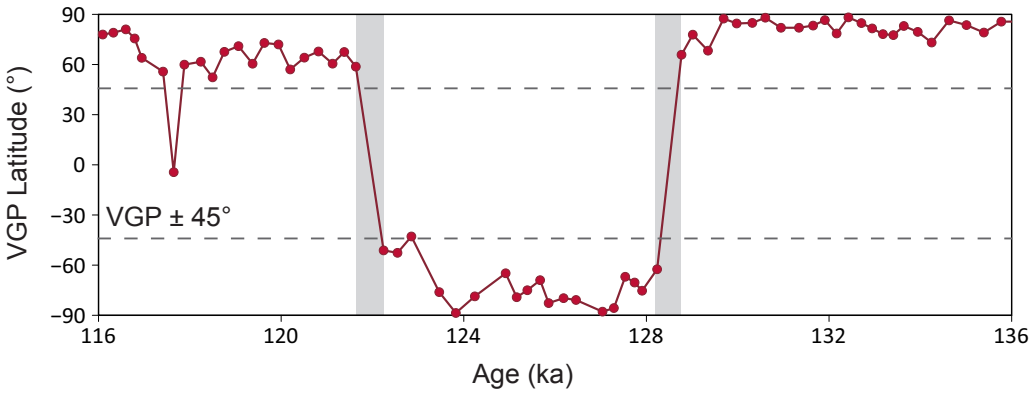

Figure 9: VGP latitude record of the Blake Excursion from ODP Site 1062E. Transition zones (VGP within ±45°) highlighted in grey.

712 Ade-Hall, J.M., Johnson, P.J., 1976. Review of Magnetic Properties of
713 Basalts and Sediments, Leg 34, in: Yeats, R.S., Hart, S.R., Ade-Hall,
714 J.M., Bass, M.N., Benson, W.E., Hart, R.A., Quilty, P.G., Sachs, H.M.,
715 Salisbury, M.H., Vallier, T.L. (Eds.), Proc. ODP, Init. Repts., Leg 34,
716 Washington (U.S. Government Printing Office). pp. 769–777.

717 Bacon, M.P., Anderson, R.F., 1982. Distribution of Thorium Isotopes Be-
718 tween Dissolved and Particulate Forms in The Deep Sea. J. Geophys. Res.
719 87, 2045–2056.

720 Banerjee, S.K., King, J., Marvin, J., 1981. A rapid method for magnetic
721 granulometry with applications to environmental studies. Geophys. Res.
722 Lett. 8, 333–336.

723 Bonhommet, N., Babkin, J., 1967. Sur la presence d'aimantation inversees
724 dans la Chaine des Puys. Compt. Rend. Acad. Sci. Paris 264, 92.

725 Brown, M.C., Holme, R., Bargery, A., 2007. Exploring the influence of

the non-dipole field on magnetic records for field reversals and excursions. Geophys. J. Int. 168, 541–550.

Chaisson, W.P., Poli, M., Thunell, R.C., 2002. Gulf Stream and Western Boundary Undercurrent variations during MIS 1012 at Site 1056, Blake-Bahama Outer Ridge. Mar. Geol. 189, 79–105.

Champion, D., Lanphere, M., Kuntz, M., 1988. Evidence for a new geomagnetic reversal from lava flows in Idaho- Discussion of short polarity reversals in the Brunhes and late Matuyama polarity chrons. J. Geophys. Res. 93, 11667–11680.

Channell, J.E.T., 2006. Late Brunhes polarity excursions (Mono Lake, Laschamp, Iceland Basin and Pringle Falls) recorded at ODP Site 919 (Irminger Basin). Earth Planet Sci. Lett. 244, 378–393.

Channell, J.E.T., Xuan, C., 2009. Self-reversal and apparent magnetic excursions in Arctic sediments. Earth Planet Sci. Lett. 284, 124–131.

Channell, J.E.T., Xuan, C., Hodell, D.A., 2009. Stacking paleointensity and oxygen isotope data for the last 1.5 Myr (PISO-1500). Earth Planet Sci. Lett. 283, 14–23.

Cheng, H., Edwards, R.L., Broecker, W.S., Denton, G.H., Kong, X., Wang, Y., Zhang, R., Wang, X., 2009. Ice age terminations. Science 326, 248–52.

Cisowski, S., Hall, F., 1997. An examination of the paleointensity record and geomagnetic excursions recorded in Leg 155 cores, in: Proc. ODP, Sci. Results, Leg 155, College Station, TX (Ocean Drilling Program). pp. 231–243.

749 Clement, B.M., 2004. Dependence of the duration of geomagnetic polarity
750 reversals on site latitude. Nature 428, 637–40.

751 Cutler, K., Edwards, R., Taylor, F., Cheng, H., Adkins, J., Gallup, C.,
752 Cutler, P., Burr, G., Bloom, A.L., 2003. Rapid sea-level fall and deep-
753 ocean temperature change since the last interglacial period. Earth Planet
754 Sci. Lett. 206, 253–271.

755 Drysdale, R.N., Hellstrom, J.C., Zanchetta, G., Fallick, a.E., Sánchez Goñi,
756 M.F., Couchoud, I., McDonald, J., Maas, R., Lohmann, G., Isola, I., 2009.
757 Evidence for obliquity forcing of glacial Termination II. Science 325, 1527–
758 31.

759 Evans, M., Heller, F., 2001. Magnetism of loess/palaeosol sequences: recent
760 developments. Earth-Sci. Rev. 54, 129–144.

761 Fang, X., Li, J., Vandervoo, R., Mac Niocaill, C., Dai, X., Kemp, R., Der-
762 byshire, E., Cao, J., Wang, J., Wang, G., 1997. A record of the Blake
763 Event during the last interglacial paleosol in the western Loess Plateau of
764 China. Earth Planet Sci. Lett. 146, 73–82.

765 Francois, R., Frank, M., Rutgers Van Der Loeff, M.M., Bacon, M.P., 2004.
766 230Th normalization: An essential tool for interpreting sedimentary fluxes
767 during the late Quaternary. Paleoceanography 19, PA1018.

768 Frank, M., Schwarz, B., Baumann, S., Kubik, P., Suter, M., Mangini, A.,
769 1997. A 200 kyr record of cosmogenic radionuclide production rate and ge-
770 omagnetic field intensity from 10Be in globally stacked deep-sea sediments.
771 Earth Planet Sci. Lett. 149, 121–129.

772 Giosan, L., Flood, R.D., Grützner, J., Franz, S.O., Poli, M.s., Hagen, S.,
773 2001. High-Resolution Carbonate Content Estimated from Diffuse Spec-
774 tral Reflectance for Leg 172 Sites, in: Keigwin, L.D., Rio, D., Acton, G.D.,
775 Arnold, E. (Eds.), Proc. ODP, Sci. Results, Leg 172, Ocean Drilling Pro-
776 gram, College Station, TX. pp. 1–12.

777 Grützner, J., Giosan, L., Franz, S.O., Tiedemann, R., Cortijo, E., Chaisson,
778 W.P., Flood, R.D., Hagen, S., Keigwin, L.D., Poli, S., Rio, D., T, W.,
779 2002. Astronomical age models for Pleistocene drift sediments from the
780 western North Atlantic (ODP Sites 1055-1063). Mar. Geol. 189, 5–23.

781 Gubbins, D., 1999. The distinction between geomagnetic excursions and
782 reversals. Geophys. J. Int. 137, F1–F4.

783 Heezen, B.C., Hollister, C.D., Ruddiman, W.F., 1966. Shaping of the Conti-
784 nental Rise by Deep Geostrophic Contour Currents. Science 152, 502–508.

785 Henderson, G., Heinze, C., Anderson, R., Winguth, a., 1999. Global distribu-
786 tion of the 230Th flux to ocean sediments constrained by GCM modelling.
787 Deep Sea Research Part I: Oceanographic Research Papers 46, 1861–1893.

788 Henderson, G.M., 2002. Seawater (234U/238U) during the last 800 thousand
789 years. Earth Planet Sci. Lett. 199, 97–110.

790 Henderson, G.M., Anderson, R.F., 2003. The U-series Toolbox for Paleo-
791 ceanography. Rev. Mineral. Geochem. 52, 493–531.

792 Henderson, G.M., Slowey, N.C., Fleisher, M.Q., 2001. U-Th dating of car-
793 bonate platform and slope sediments. Geochim. Cosmochim. Acta 65,
794 2757–2770.

795 Heslop, D., Dekkers, M.J., Kruiver, P.P., van Oorschot, I.H.M., 2002. Anal-
796 ysis of isothermal remanent magnetization acquisition curves using the
797 expectation-maximization algorithm. Geophysical Journal International
798 148, 58–64.

799 Hollerbach, R., 1993. A geodynamo model incorporating a finitely conducting
800 inner core. Phys. Earth Planet. Inter. 75, 317–327.

801 Holt, J.W., Kirschvink, J.L., 1996. Geomagnetic field inclinations for the
802 past 400 kyr from the 1-km core of the Hawaii Scientific Drilling Project.
803 J. Geophys. Res. 101, 11655–11663.

804 Kawamura, K., Parrenin, F., Lisiecki, L., Uemura, R., Vimeux, F., Sever-
805 inghaus, J.P., Hutterli, M.a., Nakazawa, T., Aoki, S., Jouzel, J., Raymo,
806 M.E., Matsumoto, K., Nakata, H., Motoyama, H., Fujita, S., Goto-Azuma,
807 K., Fujii, Y., Watanabe, O., 2007. Northern Hemisphere forcing of climatic
808 cycles in Antarctica over the past 360,000 years. Nature 448, 912–916.

809 Keigwin, L.D., Curry, W.B., Lehman, S.J., Johnsen, S., 1994. The role of
810 the deep ocean in North Atlantic climate change between 70 and 130 kyr
811 ago. Nature 371, 323–326.

812 King, J., Banerjee, S.K., Marvin, J., Özdemir, O., 1982. A comparison
813 of different magnetic methods for determining the relative grain size of
814 magnetite in natural materials: Some results from lake sediments. Earth
815 Planet Sci. Lett. 59, 404–419.

816 Knudsen, M.F., Henderson, G.M., Mac Niocaill, C., West, A.J., 2007.

817 Seven thousand year duration for a geomagnetic excursion constrained
818 by 230Thxs. Geophys. Res. Lett. 34, 1–6.

819 Knudsen, M.F., Mac Niocaill, C., Henderson, G., 2006. High-resolution data
820 of the Iceland Basin geomagnetic excursion from ODP sites 1063 and 983:
821 Existence of intense flux patches during the excursion? Earth Planet Sci.
822 Lett. 251, 18–32.

823 Korte, M., 2005. Continuous geomagnetic field models for the past 7 millen-
824 nia: 1. A new global data compilation. Geochemistry Geophysics Geosys-
825 tems 6, Q02H16.

826 Kukla, G., Heller, F., Ming, L., Chun, X., Sheng, L., Sheng, A., 1988. Pleis-
827 tocene climates in China dated by magnetic susceptibility. Geology 16,
828 811–814.

829 Laj, C., Channell, J.E., 2007. Geomagnetic Excursions, in: Schubert, G.,
830 Bercovici, D., Dziewonski, A., Herring, T., Kanamori, H., Kono, M., Ol-
831 son, P.L., Price, G.D., Romanowicz, B., Spohn, T., Stevenson, D., Watts,
832 A.B. (Eds.), Treatise on Geophysics. Geomagnetism, 5, Elsevier B.V., Am-
833 sterdam. pp. 373–416.

834 Laj, C., Kissel, C., Mazaud, A., Channell, J.E.T., Beer, J., 2000. North
835 Atlantic palaeointensity stack since 75ka (NAPIS-75) and the duration of
836 the Laschamp event. Philos.Trans. of the R. Soc. Lond. A 358, 1009–1025.

837 Laj, C., Kissel, C., Roberts, A.P., 2006. Geomagnetic field behavior during
838 the Iceland Basin and Laschamp geomagnetic excursions: A simple tran-
839 sitional field geometry? Geochemistry Geophysics Geosystems 7, 1–17.

840 Lisiecki, L.E., Raymo, M.E., 2005. A Pliocene-Pleistocene stack of 57 globally
841 distributed benthic δ 18 O records. Paleoceanography 20, PA1003.

842 Lund, S.P., Acton, G., Clement, B., Hastedt, M., Okada, M., Williams, T.,
843 1998. Geomagnetic field excursions occurred often during the last million
844 years. Eos Trans. AGU 79, 178–179.

845 Lund, S.P., Williams, T., Acton, G., Clement, B., Okada, M., 2001. Brunhes
846 Chron magnetic-field excursions recovered from Leg 172 sediments, in:
847 Keigwin, L.D., Rio, D., Acton, G.D., Arnold, E. (Eds.), Proc. ODP, Sci.
848 Results, Leg 172, Ocean Drilling Program, College Station, TX. pp. 1–18.

849 Mason, A.J., Henderson, G.M., 2010. Correction of multi-collector-ICP-MS
850 instrumental biases in high-precision uraniumthorium chronology. Int. J.
851 Mass Spectrom. 295, 26–35.

852 Ménabréaz, L., Thouveny, N., Camoin, G., Lund, S.P., 2010. Paleomagnetic
853 record of the late Pleistocene reef sequence of Tahiti (French Polynesia):
854 A contribution to the chronology of the deposits. Earth Planet Sci. Lett.
855 294, 58–68.

856 Merrill, R., McFadden, P.L., 1994. Geomagnetic field stability: Reversal
857 events and excursions. Earth Planet Sci. Lett. 121, 57–69.

858 Merrill, R.T., McFadden, P.L., 1999. Geomagnetic polarity transitions. Rev.
859 Geophys. 37, 201.

860 Nowaczyk, N.R., Frederichs, T.W., Eisenhauer, A., Gard, G., 1994. Magne-
861 tostratigraphic Data From Late Quaternary Sediments From the Yermak

Plateau, Arctic Ocean: Evidence For Four Geomagnetic Polarity Events Within the Last 170 Ka of the Brunhes Chron. Geophys. J. Int. 117, 453–471.

Osmond, J.K., Ivanovich, M., 1992. Uranium Series mobilization and surface hydrology, in: Ivanovich, M., Harmon, R.S. (Eds.), Uranium Series disequilibrium - applications to earth, marine, and environmental sciences, Oxford Science. pp. 259–289.

Parés, J.M., Van der Voo, R., Yan, M., Fang, X., 2004. After the dust settles: Why is the Blake event imperfectly recorded in the Chinese Loess?, in: Channell, J.E., Kent, D.V., Lowrie, W., Meert, J. (Eds.), AGU Geophysical Monograph Series, 145: Timescales of the Paleomagnetic Field, AGU, Washington, D.C.. pp. 191–204.

Roberts, A.P., 2008. Geomagnetic excursions: Knowns and unknowns. Geophys. Res. Lett. 35, 1–7.

Roberts, A.P., Winklhofer, M., 2004. Why are geomagnetic excursions not always recorded in sediments? Constraints from post-depositional remanent magnetization lock-in modelling. Earth Planet Sci. Lett. 227, 345–359.

Robinson, L.F., Belshaw, N.S., Henderson, G.M., 2004. U and Th concentrations and isotope ratios in modern carbonates and waters from the Bahamas. Geochim. Cosmochim. Acta 68, 1777–1789.

Schwartz, M., Lund, S.P., Hammond, D.E., Schwartz, R., Wong, K., 1997. Early sediment diagenesis on the Blake/Bahama Outer Ridge, North At-

lantic Ocean, and its effects on sediment magnetism. J. Geophys. Res. 102, 7903–7914.

Schwartz, M., Lund, S.P., Johnson, T.C., 1996. Environmental factors as complicating influences in the recovery of quantitative geomagnetic-field paleointensity estimates from sediments. Geophys. Res. Lett. 23, 2693–2696.

Shipboard Scientific Party, 1998a. Deep Blake Bahama Outer Ridge, Sites 1060, 1061, and 1062, in: Keigwin, L., Rio, D., Acton, G. (Eds.), Proc. ODP, Init. Repts., Leg 172, College Station, TX (Ocean Drilling Program). pp. 157–250.

Shipboard Scientific Party, 1998b. Explanatory Notes, in: Keigwin, L., Rio, D., Acton, G. (Eds.), Proc. ODP, Init. Repts., Leg 172, College Station TX (Ocean Drilling Program). pp. 13–29.

Smith, J.D., Foster, J.H., 1969. Geomagnetic reversal in Brunhes normal polarity epoch. Science 163, 565–567.

Tauxe, L., 1993. Sedimentary Records of Relative Paleointensity of the Geomagnetic Field: Theory and Practice. Rev. Geophys. 31, 319–354.

Tauxe, L., Kent, D.V., 2004. A Simplified Statistical Model for the Geomagnetic Field and the Detection of Shallow Bias in Paleomagnetic Inclinations : Was the Ancient Magnetic Field Dipolar?, in: Channell, J.E., Kent, D.V., Lowrie, W., Meert, J.G. (Eds.), AGU Geophysical Monograph Series, 145: Timescales of the Paleomagnetic Field, AGU, Washington, D.C.. pp. 101–115.

907 Thomas, A.L., Henderson, G.M., Deschamps, P., Yokoyama, Y., Mason,
908 A.J., Bard, E., Hamelin, B., Durand, N., Camoin, G., 2009. Penultimate
909 deglacial sea-level timing from uranium/thorium dating of Tahitian corals.
910 Science 324, 1186–1189.

911 Thomas, A.L., Henderson, G.M., McCave, I.N., 2007. Constant bottom
912 water flow into the Indian Ocean for the past 140 ka indicated by sediment
913 231Pa/230Th ratios. Paleoceanography 22, PA4210.

914 Tric, E., Laj, C., Valet, J.P., Tucholka, P., Paterne, M., Guichard, F., 1991.
915 The Blake geomagnetic event: transition geometry, dynamical character-
916 istics and geomagnetic significance. Earth Planet Sci. Lett. 102, 1–13.

917 Tucholka, P., Fontugne, M., Guichard, F., Paterne, M., 1987. The Blake
918 magnetic polarity episode in cores from the Mediterranean Sea. Earth
919 Planet Sci. Lett. 86, 320–326.

920 Valet, J.P., Meynadier, L., Guyodo, Y., 2005. Geomagnetic dipole strength
921 and reversal rate over the past two million years. Nature 435, 802–805.

922 Valet, J.P., Plenier, G., 2008. Simulations of a time-varying non-dipole field
923 during geomagnetic reversals and excursions. Phys. Earth Planet. Inter.
924 169, 178–193.

925 Valet, J.P., Plenier, G., Herrero-Bervera, E., 2008. Geomagnetic excursions
926 reflect an aborted polarity state. Earth Planet Sci. Lett. 274, 472–478.

927 Vandamme, D., 1994. A new method to determine paleosecular variation.
928 Phys. Earth Planet. Inter. 85, 131–142.

929 Zhu, R., Coe, R.S., Guo, B., Anderson, R., Zhao, X., 1998. Inconsistent
930 palaeomagnetic recording of the Blake event in Chinese loess related to
931 sedimentary environment. Geophys. J. Int. 134, 867–875.

932 Zhu, R., Pan, Y., Coe, R.S., 2000. Paleointensity studies of a lava succession
933 from Jilin Province, northeastern China: Evidence for the Blake event. J.
934 Geophys. Res. 105, 8305–8317.

935 Zhu, R., Zhou, L., Laj, C., Mazaud, A., Ding, Z., 1994. The Blake geomag-
936 netic polarity episode recorded in Chinese loess. Geophys. Res. Lett. 21,
937 697–697.

938 Ziegler, L.B., Constable, C.G., Johnson, C.L., Tauxe, L., 2011. PADM2M: a
939 penalized maximum likelihood model of the 0-2 Ma palaeomagnetic axial
940 dipole moment. Geophys. J. Int. 184, 1069–1089.